Ascent Performance Issues of a Vertical-Takeoff Rocket Launch Vehicle

Richard W. Powell,* J. Christopher Naftel,* and Christopher I. Cruz*
NASA Langley Research Center, Hampton, Virginia 23665

Advanced manned launch systems studies under way at the NASA Langley Research Center are part of a broader effort that is examining options for the next manned space transportation system to be developed by the United States. One promising concept that uses near-term technologies is a fully reusable, two-stage vertical-takeoff rocket vehicle. This vehicle features parallel thrusting of the booster and orbiter with the booster cross-feeding the propellant to the orbiter until staging. In addition, after staging, the booster glides back unpowered to the launch site. This study concentrated on two issues that could affect the ascent performance of this vehicle. The first is the large gimbal angle range required for pitch trim until staging because of the propellant cross-feed. Results from this analysis show that if control is provided by gimballing of the rocket engines, they must gimbal greater than 20 deg, which is excessive when compared with current vehicles. However, this analysis also showed that this limit could be reduced to 10 deg if gimballing were augmented by throttling the booster engines. The second issue is the potential influence of off-nominal atmospheric conditions (density and winds) on the ascent performance. This study showed that a robust guidance algorithm could be developed that would insure accurate insertion, without prelaunch atmospheric knowledge.

Nomenclature

$C1$ = constant in commanded pitch angle polynomial, deg/s
$C2$ = constant in commanded pitch angle polynomial, deg/s^2
h = altitude, m
K_q = pitch rate error gain, s
K_α = angle of attack error gain, n.d.
q = pitch rate, deg/s
$\text{time}_{\text{init}}$ = time the predictor-corrector algorithm is invoked, s
V_I = inertial velocity, m/s
α = angle of attack, deg
α_c = commanded angle of attack, deg
ΔG_{rad} = change in geocentric radius at orbital insertion as compared with optimal trajectory, m
$\Delta\text{Payload}$ = change in delivered payload as compared to optimal trajectory, kg
ΔTime = change in orbital insertion time as compared with optimal trajectory (positive longer), s
ΔV_{aero} = velocity loss increment due to aerodynamics, m/s
ΔV_{circ} = ΔV required to circularize, m/s
ΔV_{cor} = velocity loss increment due to Coriolis effect, m/s
ΔV_{grav} = velocity loss increment due to gravity, m/s
ΔV_{ideal} = ideal velocity increment, m/s
ΔV_{loss} = total velocity loss increments, m/s
ΔV_{thrust} = velocity loss increment due to reduced thrust induced by atmospheric pressure, m/s
ΔV_{tv} = velocity loss increment due to thrust vector misalignments, m/s
$\Delta\gamma$ = change in flight-path angle at orbital insertion as compared with optimal trajectories, deg
δ_e = elevator deflection (positive down), deg
δ_{e_c} = commanded elevator deflection (positive down), deg
δ_{e_i} = initial elevator deflection (positive down), deg
δi_p = engine pitch gimbal angle (positive up), deg
δi_y = engine yaw gimbal angle (positive left), deg
Θ_c = commanded pitch angle, deg
Θ_{init} = pitch angle when predictor-corrector guidance algorithm is invoked, deg
ρ = atmospheric density, kg/m^3
ρ_{76} = 1976 standard atmospheric density, kg/m^3
σ = standard deviation, n.d.

Introduction

EARTH-to-orbit space transportation concepts have been studied for many years to fulfill a variety of anticipated mission needs.[1-4] The primary objectives have been to define vehicles that both substantially reduce the cost of manned space transportation and provide a complement to a transportation architecture to support a wide range of scientific, military, and commercial uses. These studies have identified concepts using both near-term and more advanced technology. One of the promising concepts with near-term technology is a fully reusable, two-stage, all-rocket vehicle with parallel thrusting (both the orbiter and the booster thrust from liftoff to staging) and propellant cross-feed from the booster to the orbiter. After staging at Mach 3, the booster glides back to the launch site unpowered. Because this vehicle employs features that have not been utilized to date, a detailed analysis of the ascent was conducted.

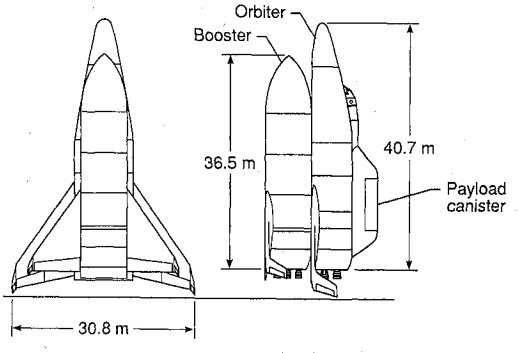

Fig. 1 Vertical-takeoff rocket vehicle.

Received March 28, 1990; revision received June 25, 1990; accepted for publication June 25, 1990.

*Aerospace Engineer, Vehicle Analysis Branch, Space Systems Division. Member AIAA.

Table 1 Characteristics of vertical-takeoff rocket vehicle

Parameter	Booster	Orbiter
Gross mass, kg	453,742	538,361
Dry mass, kg	48,699	69,387
Payload, kg		9,100
Number of engines	6	4
Engine vacuum thrust, N	1.557×10^6	1.557×10^6
Engine vacuum I_{sp}, s	438	438
Wing reference area, m^2	144	185

Specifically, this paper discusses the optimal ascent flight profile for this vehicle, control of the vehicle during ascent comparing the techniques of using engine gimbal alone with engine gimbal combined with throttling, design of a guidance algorithm to aid in the evaluation of off-nominal atmospheric conditions (density profiles and winds), and the results of simulations with these off-nominal conditions.

Vehicle Description

The all-rocket vehicle (Fig. 1) used for this study was taken from the advanced manned launch system vehicle studies currently under way.[2] Table 1 shows its major characteristics. This vehicle is composed of an unmanned booster and a manned orbiter. The unmanned booster stages at Mach 3 and performs an unpowered glide to the launch site. Mach 3 was chosen for staging for two major reasons. The first is that this is the highest Mach number that would allow an unpowered return to the launch site after staging with adequate performance reserves. The second is that at this low Mach number, no thermal protection system is required.[1] Both the booster and the orbiter engines use liquid hydrogen (LH_2) and liquid oxygen (LOX) as propellants. The orbiter engines use propellants cross-fed from the booster until staging and an internal propellant for the remainder of the ascent.

Aerodynamics

The aerodynamic data base for both vehicles was generated using the aerodynamic preliminary analysis system (APAS).[5,6] APAS is an interactive computer code that predicts the aerodynamic characteristics of a vehicle from subsonic to hypersonic speeds using a common geometric definition. APAS incorporates a variety of engineering techniques to estimate the basic longitudinal and lateral-directional characteristics of aerospace vehicles as well as control effectiveness and dynamic derivatives. Slender body, vortex panel, wave drag, and viscous drag methods are used in the subsonic to low supersonic speed regime. At the higher speeds, tangent-cone, tangent-wedge, and reference enthalpy methods are utilized to approximate the pressure and shear stress distributions on the vehicle. The APAS program has been used on many previous vehicles, and through comparisons with wind-tunnel and flight data, it has been shown to give results accurate to the fidelity required for this study.

Atmospheric Profile Modeling

Off-nominal atmospheric conditions, both density and wind profiles, were used to evaluate the effectiveness of the guidance algorithm. The first off-nominal conditions used were constant bias factors between 0.8 and 1.2 applied to the standard atmospheric density, which, for these studies, is the 1976 standard atmosphere.[7] To simulate a more realistic variation in atmospheric density, density profiles were generated using the global reference atmosphere model (GRAM).[8] The GRAM was developed to provide realistic worldwide atmospheric data including winds. The GRAM can be used to generate the monthly mean and perturbation data. A total of 41 simulations were generated. These are as follows: 1) nominal 1976 atmosphere with no winds; 2) factors of 0.8, 0.9, 1.1, and 1.2 applied to nominal 1976 atmosphere with no winds; 3) monthly mean data with no winds; 4) monthly mean data with winds; 5) 10 perturbed atmospheres with winds for selected date (July 1, 1989); and 6) 3 σ data for selected date (July 1, 1989). Figures 2–4 show the range of atmospheric density and wind profiles generated by GRAM and used in this study.

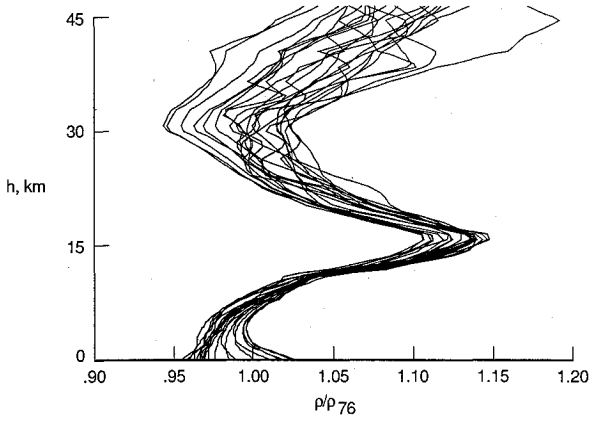

Fig. 2 Atmospheric density profiles calculated by GRAM.

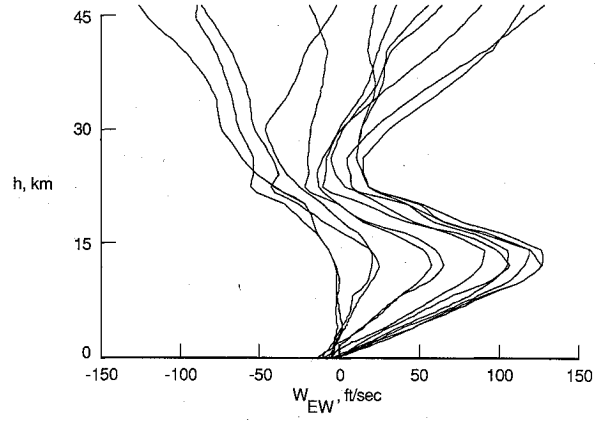

Fig. 3 East-west wind components calculated by GRAM.

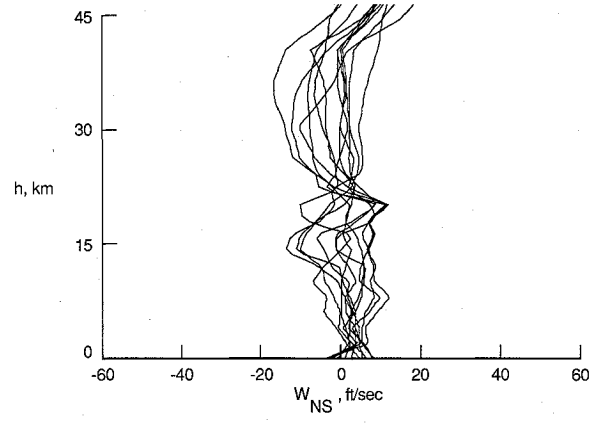

Fig. 4 North-south wind components calculated by GRAM.

Trajectory Simulations

All of the trajectories presented in this paper were generated by the three-degree-of-freedom version of the program to optimize simulated trajectories (POST).[9] POST is a generalized event-oriented trajectory program that can be used to analyze ascent, on-orbit, and entry trajectories. POST can be used to optimize any calculated variable that may be subjected to a combination of both equality and inequality constraints.

The program has been modified to include a predictor-corrector guidance capability, which should be representative

of the state-of-the-art guidance algorithms available when this vehicle would be built. The predictor-corrector capability was implemented by including a three-degree-of-freedom simulation as an inner loop to the main simulation. This allows the predictor-corrector guidance model to have nominal environmental characteristics (planet, atmosphere, gravity, aerodynamic, propulsion, weights, etc.) and the main simulation to have perturbed characteristics. For this study, identical models, with the exception of the atmosphere, were used by both the main simulation and the predictor-corrector guidance algorithm. The predictor-corrector guidance models used only the 1976 standard atmosphere. The predictor-corrector models were not provided any atmospheric dispersions or winds information.

Design Trajectory

The design trajectory was a due east launch from the NASA Kennedy Space Center that inserted into a 95- × 185-km orbit and circularized at apogee. The trajectory maximized the inserted payload subject to imposed constraints. These design constraints included a maximum dynamic pressure limit of 40 kPa, a maximum wing normal force of $\pm 2.15 \times 10^6$ N for the orbiter, and $\pm 1.25 \times 10^6$ N for the booster. The additional constraints were that staging would occur at Mach 3, with an altitude greater than 24 km and an angle of attack between -6 and 2 deg. This minimum altitude constraint was designed to provide adequate performance reserves for the booster glide back. The angle-of-attack limitation was imposed as a result of the staging analysis. The optimal ascent trajectory for the vertical-takeoff rocket vehicle from launch to orbital insertion is shown in Fig. 5.

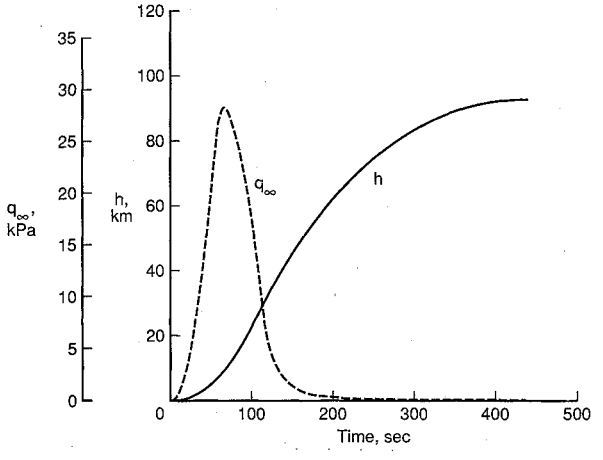

a) Dynamic pressure and altitude histories

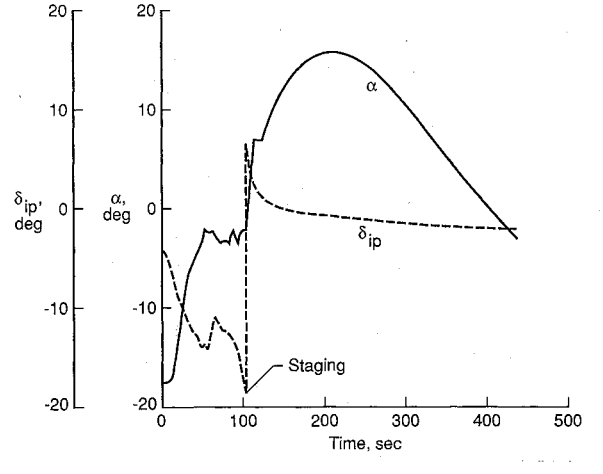

b) Engine pitch gimbal angle and angle-of-attack histories

Fig. 5 Optimal ascent trajectory for vertical-takeoff vehicle.

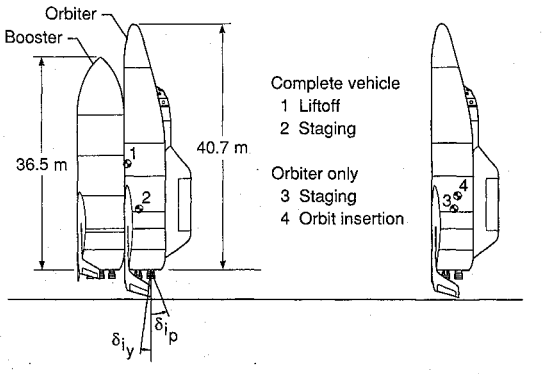

Fig. 6 Center-of-gravity history during ascent of vertical-takeoff rocket.

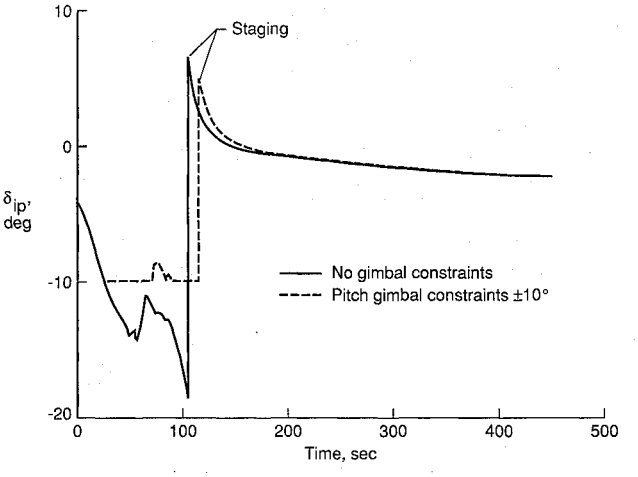

a) Engine pitch gimbal angle history

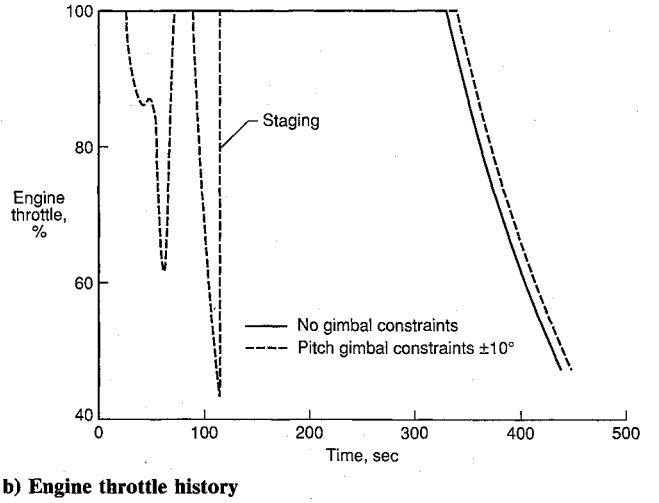

b) Engine throttle history

Fig. 7 Control history comparison of vertical-takeoff rocket vehicle with and without gimbal angle limits.

Examination of this optimal ascent under nominal conditions shows large gimbal angle requirements to be a vehicle design issue. Because this vehicle is a two-stage concept that employs parallel burn and cross-feed, it will have a large lateral center-of-gravity shift during ascent until staging. Figure 6 shows the center-of-gravity movement of this vehicle. As fuel is used from liftoff to staging, the center of gravity moves aft and into the orbiter, causing the gimbal angle required for trimming to move from -4 deg at liftoff to -18 deg just prior to staging. After staging, the gimbal angle of the orbiter is 7 deg and is reduced to about 0 deg at orbital insertion.

Gimbal Angle Reduction

Because the optimal trajectory under nominal atmospheric density and with no winds showed the need for large engine gimbal angles, an alternate control technique was developed. This technique was to augment the control provided by gimballing with throttling of the booster engines. To illustrate this technique, another optimal trajectory was determined that had a maximum allowable gimbal angle limit of ±10 deg. To provide the additional required pitch control, the booster engines were throttled when the engines reached this gimbal limit. After staging, the engines remain within the 10 deg limit. The comparison trajectories are shown in Fig. 7, and Table 2 compares the ascent performance of the vehicle using all gimbal control and the vehicle using both gimballing and throttling for control. For this study, all of the booster engines were throttled equally. In actual practice, engines would be shut down to avoid the deep throttling required for trim near staging. The use of this control technique results in a reduction in inserted weight of 1288 kg. This translates in a minor resizing of the booster to accommodate a 0.3% increase in required propellant.

Table 2 Comparison of rocket vehicle with and without engine gimbal constraints

Parameter	Without gimbal constraints	Pitch gimbal angles limited to ±10 deg
ΔV, m/s	9334	9381
ΔV_{loss}, m/s	1872	1918
ΔV_{thurst}, m/s	200	211
ΔV_{aero}, m/s	193	194
ΔV_{grav}, m/s	1327	1342
ΔV_{tv},m/s	156	175
ΔV_{cor}, m/s	−4	−4
ΔV_{circ}, m/s	26	26
Time to staging, s	104.8	114.4
Time to insertion, s	438.3	449.5

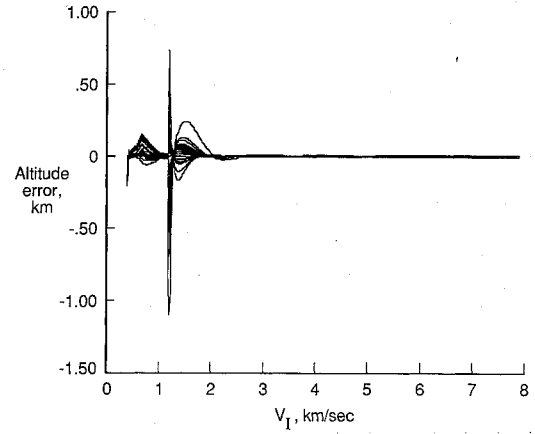

Fig. 8 Altitude error histories for all trajectories simulated for vertical-takeoff rocket vehicle.

Guidance Algorithm

To determine the impact of off-nominal atmospheric conditions on the ascent performance of this vehicle, a guidance algorithm had to be developed. This guidance algorithm was divided into two parts. In the first part, the vehicle was commanded to fly to a reference trajectory that was defined by an altitude velocity relationship. At 350 s into the trajectory (≅ 100 s before orbital insertion), the guidance algorithm switched to a predictor-corrector algorithm to ensure accurate insertion. The predictor-corrector guidance algorithm, which is very compute intensive, was not required during the early portion of the ascent. This algorithm determined the linear and quadratic coefficients of a polynomial that described the commanded pitch attitude $[(\Theta_c = \Theta_{init} + C1(\text{time} - \text{time}_{init}) + C2(\text{time} - \text{time}_{init})^2]$. This predictor-corrector algorithm was utilized to update the control history at 10-s intervals until orbital insertion. The predictor-corrector

Table 3 Vertical-takeoff rocket simulation results for constant factor atmospheric density variations

Parameter	Factor = 0.8	Factor = 0.9	Factor = 1.1	Factor = 1.2
ΔPayload, kg	782	464	−849	−3452
ΔTime, s	−1.1	−0.7	1.2	5.1
ΔG_{rad}, m	−0.6	−0.15	0.2	−0.03
$\Delta\gamma$, deg	−0.0003	−0.0001	0.0003	−0.0001

Table 4 Vertical-takeoff rocket simulation results for GRAM atmospheric density variations (monthly mean density with no winds)

Parameter	January	February	March	April	May	June	July	August	September	October	November	December
ΔPayload, kg	−254	−208	−225	−277	−339	−416	−254	−208	−225	−277	−339	−416
ΔTime, s	0.4	0.3	0.3	0.4	0.5	0.6	0.4	0.3	0.3	0.4	0.5	0.6
ΔG_{rad}, m	0.44	0.03	0.24	0.15	0.12	0.06	0.44	0.03	0.24	0.15	0.12	0.06
$\Delta\gamma$, deg	0.0004	0.0002	0.0003	0.0004	0.0003	−0.0001	0.0004	0.0002	0.0003	0.0004	0.0003	−0.0001

Table 5 Vertical-takoff rocket simulation results for GRAM atmospheric density variations (monthly mean density with winds)[a]

Parameter	January	February	March	April	May	June	July	August	September	October	November	December
ΔPayload, kg	211	270	240	118	−102	−357	−565	−545	−39	−137	54	160
ΔTime, s	−0.3	0.4	−0.4	−0.2	0.1	0.5	0.7	0.7	0.6	0.2	−0.1	0.3
ΔG_{rad}, m	1.2	0.3	−0.5	−0.6	−0.3	−0.3	−0.2	−0.1	0.9	1.2	0.60	1.2
$\Delta\gamma$, deg	0.0006	−0.0001	−0.0003	−0.0004	−0.0003	−0.0006	−0.0001	0.0001	−0.0001	−0.0003	−0.0005	−0.0003

[a]See Figs. 3 and 4 for wind profiles.

Table 6 Vertical-takeoff rocket simulation results for GRAM atmospheric density variations (perturbations for July 1, 1989, with winds)[a]

Parameter	Pert 1	Pert 2	Pert 3	Pert 4	Pert 5	Pert 6	Pert 7	Pert 8	Pert 9	Pert 10	$+3\sigma$ Pert	-3σ Pert
ΔPayload, kg	−685	−570	−637	−642	−645	−634	−635	−601	−594	−536	−1204	−152
Δ Time, s	1.0	0.8	0.9	0.9	0.9	0.9	0.9	0.9	0.9	0.8	1.7	0.2
ΔG_{rad}, m	−10.4	−10.3	−10.7	−10.4	−10.2	−10.5	−10.5	−10.4	−10.6	−10.3	−0.4	−0.1
$\Delta\gamma$, deg	0.0004	0.0006	−0.0003	−0.0003	0.0005	0.0002	−0.0002	0.0003	0.0003	0.0002	−0.002	0.001

[a]See Figs. 3 and 4 for wind profiles.

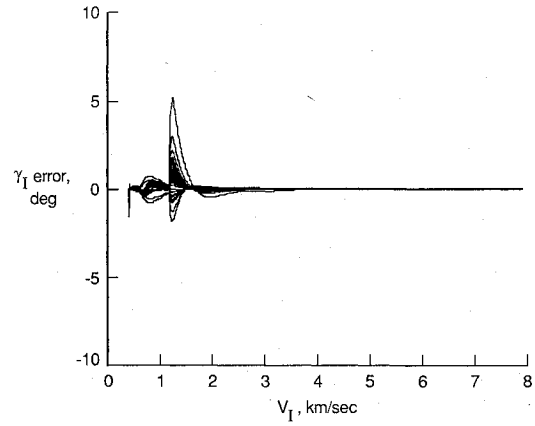

Fig. 9 Flight-path angle error histories for all trajectories for vertical-takeoff rocket vehicle.

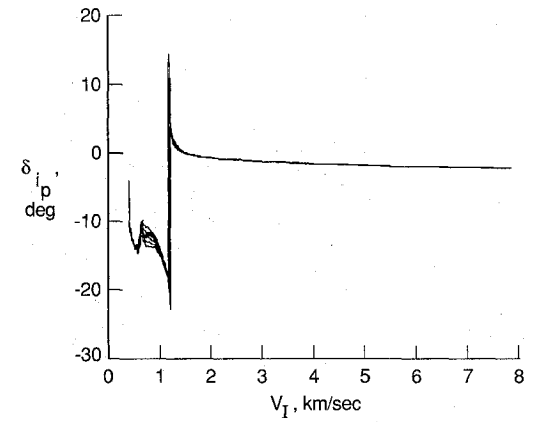

Fig. 10 Engine pitch angle histories for all trajectories simulated for vertical-takeoff rocket vehicle.

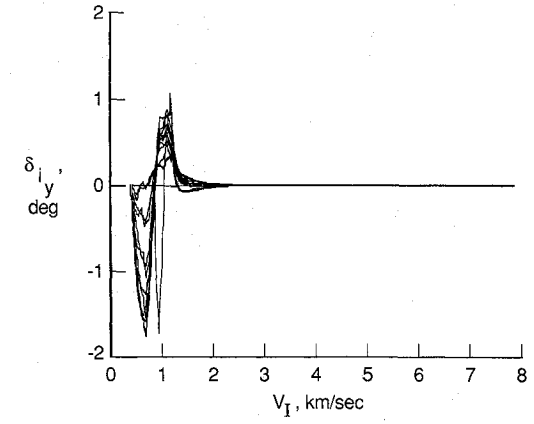

Fig. 11 Engine yaw angle histories for all trajectories simulated for vertical-takeoff rocket vehicle.

algorithm used three-degree-of-freedom equations that were modified to include longitudinal static trim.

Simulation Results

The ascent trajectory analysis included simulations involving off-nominal atmospheric conditions. The first off-nominal conditions used in the flight control sensitivity analysis were constant bias factors applied to the standard atmospheric density. The off-nominal densities were simulated by applying factors of 0.8–1.2 to the standard density. The results of these cases are shown in Table 3. The results of the simulations that used the GRAM-generated atmospheres are shown in Table 4. Simulations were also conducted with these same GRAM atmospheric density profiles with winds added. The results of these simulations are shown in Table 5. In addition, trajectories were simulated using 10 perturbed profiles for a single date (July 1, 1989). The results of these simulations and those with a $\pm 3\sigma$ variation in the mean density for this same date are shown in Table 6. All of the inserted payload capability variation fell within the limits established by the constant density factors, namely, -3452–782 kg. The results of these simulations require that the orbiter be resized to accommodate a 0.7% increase in required propellant. The predictor-corrector guidance algorithms provided for accurate insertions with errors in geocentric radius at insertion of <11 m for all cases. Figure 8 shows the altitude error and Fig. 9 shows the flight-path angle error for all of the cases simulated. Note that while there are significant errors in both altitude and flight-path angle prior to staging, the guidance algorithm assures accurate orbital insertion. Figures 10 and 11 show the gimbal angle histories for these cases. These figures show the influence of the winds on the trajectories. One important issue that can be seen in Fig. 10 is that the pitch gimbal angle requirements increased from -18 deg nominally to -22 deg with winds. This increased gimbal angle requirement emphasizes the need for an alternative to pure gimbal angle control.

Summary

A study has been conducted that investigated some of the ascent issues that could influence the design of a fully reusable two-stage, vertical-takeoff, all-rocket vehicle that employs parallel burning with propellants cross-fed from the booster to the orbiter until staging. Two issues were identified. The first was the large gimbal angle requirement to control the vehicle just prior to staging. This is due to the center of gravity moving aft and into the orbiter as the propellant is depleted from the booster. If gimballing alone is used for control, this requires gimbal angles in excess of 20 deg. However, the study showed that for a 0.3% propellant increase in the booster, this gimbal angle requirement can be reduced to 10 deg by supplementing the gimballing with throttling of the booster engines. The second issue was the impact on the ascent performance of off-nominal atmospheric density profiles and winds. The results indicate that these off-nominal conditions require that the orbiter be resized to accommodate a 0.7% increase in propellant.

References

[1]Freeman, D. C., et al., "The Future Space Transportation System (FSTS) Study," *Astronautics and Aeronautics*, Vol. 21, No. 6, 1983, pp. 36–56, 62.

[2]Talay, T. A., and Morris, W. D., "Advanced Manned Launch Systems," European Aerospace Conference, Paper EAC '89-17, May 1989.

[3]Piland, W. M., and Talay, T. A., "Advanced Manned Launch Systems Comparisons," International Astronautical Federation, Paper 89-121, Oct. 1989.

[4]Martin, J. A., et al., "Orbit on Demand: In This Century If Pushed," *Astronautics and Aeronautics*, Vol. 23, No. 2, 1985, pp. 46–61.

[5]Divan, P., "Aerodynamic Preliminary Analysis System II, Part II—User's Manual," NASA CR-165628, April 1981.

[6]Cruz, C., and Wilhite, A., "Prediction of High Speed Aerodynamic Characteristics Using the Aerodynamic Preliminary Analysis System," AIAA Paper 89-2173, July 1989.

[7]*U.S. Standard Atmosphere, 1976*. National Oceanic and Atmospheric Administration, NASA, and United States Air Force, Washington, DC, Oct. 1976.

[8]Justus, C. G., Fletcher, G. R., Gramling, F. E., and Pace, W. B., "The NASA/MSFC Global Reference Atmospheric Model—Mod 3 (With Spherical Harmonic Wind Model)," NASA CR-3256, 1980.

[9]Brauer, G. L., Cornick, D. E., and Stevenson, R., "Capabilities and Applications of the Program to Optimize Simulated Trajectories (POST)," NASA CR-2770, Feb. 1977.

James A. Martin
Associate Editor